The chemical speciation of iron in the north-east Atlantic Ocean

Boye, Marie; Aldrich, Annette; Berg, Constant M.G. van den; Jong, Jeroen T.M. de; Nirmaier, Hans; Veldhuis, Marcel; Timmermans, Klaas R.; Baar, Hein J.W. de

Published in:
Deep Sea Research Part I: Oceanographic Research Papers

DOI:
10.1016/j.dsr.2005.12.015

Document Version
Publisher's PDF, also known as Version of record

Publication date:
2006

Available online at www.sciencedirect.com
SCIENCE DIRECT
Deep-Sea Research I 53 (2006) 667–683
DEEP-SEA RESEARCH PART I
www.elsevier.com/locate/dsr

The chemical speciation of iron in the north-east Atlantic Ocean

Marie Boye[a], Annette Aldrich[a], Constant M.G. van den Berg[a,*], Jeroen T.M. de Jong[b], Hans Nirmaier[a], Marcel Veldhuis[b], Klaas R. Timmermans[b], Hein J.W. de Baar[b]

[a]*Department of Earth and Ocean Sciences, University of Liverpool, Liverpool L69 3GP, UK*
[b]*Royal Netherlands Institute for Sea Research, P.O. Box 59, 1790 AB Den Burg, Texel, The Netherlands*

Received 11 May 2004; received in revised form 13 June 2005; accepted 19 December 2005
Available online 23 March 2006

Abstract

The distribution of dissolved iron and its chemical speciation (organic complexation and redox speciation) were studied in the northeastern Atlantic Ocean along 23°W between 37 and 42°N at depths between 0 and 2000 m, and in the upper-water column (upper 200 m) at two stations further east at 45°N10°W and 40°N17°W in the early spring of 1998. The iron speciation data are here combined with phytoplankton data to suggest cyanobacteria as a possible source for the iron binding ligands. The organic Fe-binding ligand concentrations were greater than that of dissolved iron by a factor of 1.5–5, thus maintaining iron in solution at levels well above it solubility. The water column distribution of the organic ligand indicates in-situ production of organic ligands by the plankton (consisting mainly of the cyanobacteria *Synechococcus* sp.) in the euphotic layer and a remineralisation from sinking biogenic particles in deeper waters. Fe(II) concentrations varied from below the detection limit (<0.1 nM) up to 0.55 nM but represented only a minor fraction of 0% to occasionally 35% of the dissolved iron throughout the water column. The water column distribution of the Fe(II) suggests biologically mediated production in the deep waters and photochemical production in the euphotic layer. Although there was no evidence of iron limitation in these waters, the aeolian iron input probably contributed to a shift in the phytoplankton assemblage towards increased *Synechococcus* growth.

Keywords: Iron; Organic ligands; Iron speciation; Atlantic Ocean

1. Introduction

Iron limits primary productivity in a major part of the global ocean (Behrenfeld and Kolber, 1999; Coale et al., 1996). However, the chemical speciation of iron and its distribution and effects on uptake by microorganisms are not yet fully understood. Dissolved iron tends to be strongly complexed by organic ligands (Gledhill and van den Berg, 1994; Rue and Bruland, 1995, 1997; Van den Berg, 1995; Boye et al., 2001) which are thought to enhance the otherwise very low (0.1 nM) iron solubility (Wu et al., 2001). In spite of the strong organic complexation, there is evidence that iron can occur as Fe(II) in the upper water column (Waite et al., 1995; Zhuang et al., 1995) and in surface waters over the continental shelf (Boye

*Corresponding author. Tel.: +44 151 794 4096; fax: +44 151 794 4099.
E-mail address: vandenberg@liverpool.ac.uk (C.M.G. van den Berg).

0967-0637/$ - see front matter © 2006 Elsevier Ltd. All rights reserved.
doi:10.1016/j.dsr.2005.12.015

et al., 2003). Previous studies of the speciation of iron in the oceanic water column have tended to ignore its redox speciation, and these have been determined together only once before in waters along a surface transect of the Atlantic (Boye et al., 2003). It has not yet been established which form of iron (organically complexed Fe(III), inorganic Fe(III), or Fe(II)) is bioavailable (Timmermans et al., 2001). The various chemical forms of iron may, on the other hand, have taxon-specific bioavailability. It is possible, for example, that prokaryotic and eukaryotic species have different abilities to obtain iron bound to organic chelators (Hutchins et al., 1999).

The iron cycle in the North Atlantic Ocean is still poorly understood. Dissolved iron concentrations in surface waters of the North Atlantic are probably spatially and temporally highly variable, due to episodic deposition of Saharan dust (Duce and Tindale, 1991; Jickells and Spokes, 2001; de Jong et al., 2000), hydrographic features, such as fronts and eddies (de Jong et al., 2000), and biological activity. The distribution of dissolved iron in the water column of the northeast Atlantic Ocean has been studied before (Landing et al., 1995; Martin et al., 1993; Wu et al., 2001; de Jong et al., 2000; Laës et al., 2003). However, much less is known about the speciation of dissolved iron. The extent of organic complexation of iron has been determined in the north-east Atlantic (Gledhill and van den Berg, 1994; Wu et al., 2001; Boye et al., 2003), in the north-western Atlantic (Wu and Luther, 1995; Witter and Luther, 1998) and in the south and equatorial Atlantic (Powell and Donat, 2001). The distribution of Fe(II) has been determined only in surface waters of the north-east Atlantic (Boye et al., 2003). Because of the high atmospheric inputs to the north-east Atlantic Ocean (Duce and Tindale, 1991), iron is not expected to be a limiting factor of phytoplankton growth in this area. However, it has been suggested that iron may regulate export production in oligotrophic regions of the ocean (DiTullio et al., 1993; Young et al., 1991) primarily limited by nitrate levels such as in the North Atlantic central gyre. Recently, incubation experiments demonstrated that relatively high dissolved-iron concentrations in surface waters (e.g. 0.4 nM) act, in concert with limitation by major nutrients, as an important factor controlling phytoplankton growth, phytoplankton community structure and nutrient drawdown in the north-eastern Atlantic Ocean (Blain et al., 2004).

This work describes the organic complexation and redox speciation of iron in the water column of the NE Atlantic relative to the abundance of phytoplankton and the prevailing hydrography, atmospheric iron supply and biogeochemical and photochemical processes.

2. Sampling and analytical procedures

2.1. Sampling

Samples were collected during the MERLIM'98 cruise, which took place during early spring (March 1998) on board the Research Vessel *Pelagia* (cruise 64 PE 114) in the eastern North Atlantic Ocean. Four stations were sampled at depths between 0 and 2000 m, at 23°W between 42 and 37°N, and two stations further east were sampled in the upper-water column (0–200 m) at 45°N/10°W and 40°N/17°W. The station locations are shown in Fig. 1. Two stations were sampled at nearly the same position (St. 6 and 10, see Fig. 1), but at 7 days interval, to see if changes occurred over a brief time interval.

Samples from the water column were collected with 10 pre-cleaned 12 L Go-Flo bottles on a Kevlar wire. The samples were collected during a shallow cast from 10 down to 200 m and a deep cast from 250 down to 2000 m. The Go-Flo samples were closed by means of Teflon messengers and after retrieval directly stored in a clean Class 100 container. Samples were filtered over 0.2 μm polycarbonate membrane filters (Poretics) at a nitrogen pressure of 0.5 bar, and the filtered seawater was collected in clean polyethylene bottles. Subsamples were filtered directly into 30 mL sample vials (Sterilins) containing bipyridyl to stabilize Fe(II) (Boye et al., 2003); thus the exposure time of the samples after their release from the closed sample bottle was minimized to around 1 min.

The chemical speciation was carried out on-board ship, in a Class 100 container, within 1–2 days of sample collection; samples were stored in a refrigerator at ~4 °C until analysis. Sub-samples for Fe(II) determination were taken immediately after opening of the Go-Flo bottle by running filtered water into two 30 mL Sterilin tubes, of which one already contained bipyridyl to fix the Fe(II). Voltammetric analysis of the Fe(II) speciation was undertaken immediately.

Phytoplankton numbers and species composition were determined by flow cytometry (Coulter

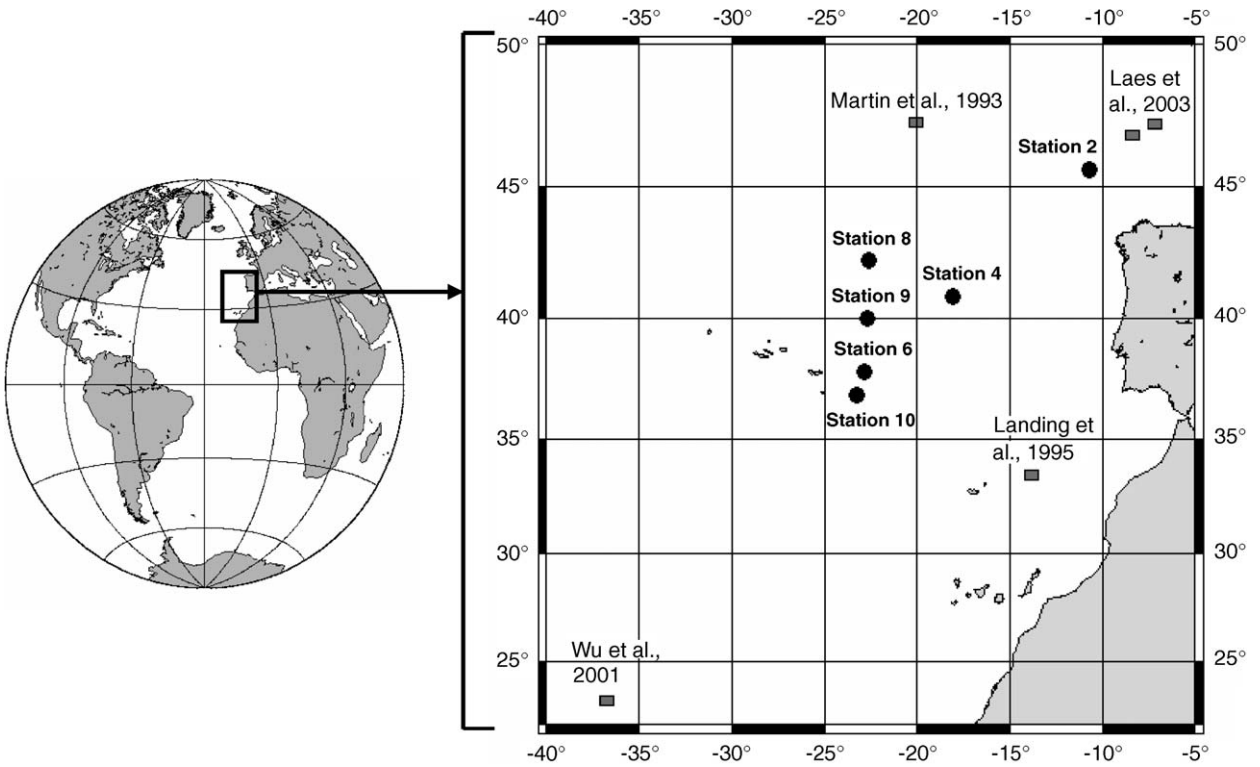

Fig. 1. Map of the sampling locations for the St 2, 4, 6, 8, 9, 10 (the positions are shown in Table 1) and for five stations from previous studies (47°N20°W: Martin et al., 1993; 34°N13°W: Landing et al., 1995, 46°26′N6°59′W (St. 27) and 46°8°W (St. 28): Laës et al., 2003; 22.8°N36.8°W: Wu et al., 2001).

XL-MCL), excitation wavelength 488 nm. Phytoplankton was separated from other particles based on the chlorophyll signal (Long Pass 610 nm). In addition, phycoerythrin (PE) containing species (*Synechococcus* sp.) were assigned using the fluorescent signal of this pigment in the 550–590 nm region (Band Pass 575 ± 20 nm) (Veldhuis and Kraay, 2004).

2.2. Analytical procedures

2.2.1. Reagents

Milli-Q-water (''MQ'', resistance 18.2 MΩ) was used for reagent preparation and for rinsing. Hydrochloric acid, ammonia and methanol (Merck, AnalaR grade) were purified by sub-boiling distillation using a quartz, cold-finger, distillation unit. The pH of a 1 M solution of HEPPS buffer (*N*-2-hydroxylethylpiperazine-*N*′-3-propanesulphonic acid, BDH product) was adjusted with ammonia to give pH 8 when diluted 100-fold with seawater. Contaminating trace metals were removed by equilibration with 50 μM manganese oxide followed by filtration (0.2 μm). A 0.02 M 1-nitroso-2-naphtol (NN) solution in methanol was used without further purification. A stock solution of 0.4 M potassium bromate (AnalaR product) was prepared in MQ and cleaned by equilibration with NN (20 μM) at pH 8 (using HEPPS, 5 mM), followed by extraction using a Sep-Pak C18 cartridge (activated with methanol). For the indirect determination of Fe(II) a 2 mM Bp (2,2-bipyridyl) solution was prepared in 0.01 M HCl. A stock solution of 10^{-6} M Fe(III), was prepared in 0.01 M hydrochloric acid, using a standard iron solution (BDH SpectrosoL); this solution also contained 2.8 mM nitric acid.

2.2.2. Equipment

An Autolab voltammeter (Eco Chemie, The Netherlands) was used for the voltammetric analyses, in conjunction with a Metrohm (Herisau, Switzerland) 663 VA electrode stand (in the hanging mercury drop mode, drop size approximately 0.5 mm^2). The reference electrode was double-junction Ag/saturated AgCl in 3 M KCl/3 M KCl, and the counter electrode was glassy carbon. During the adsorption step solutions were stirred by a

PTFE rod rotating at 2500 rpm. The voltammeter was controlled by an IBM-AT compatible computer.

2.2.3. Determination of iron speciation

Iron was determined by catalytic cathodic stripping voltammetry (CSV) using bromate as oxidant (Aldrich and van den Berg, 1998). Dissolved iron was determined by CSV using 10 μM NN after UV-digestion at the original seawater pH. The UV-digestion of the sample for at least 90 min (without acidification) has been shown to efficiently destroy the iron-binding capacity of the dissolved organic ligands (Rue and Bruland, 1997; Aldrich and van den Berg, 1998). To calibrate the accuracy of this method, an intercomparison excercise for dissolved iron was conducted comparing the dissolved Fe concentrations measured by CSV (in UV-digested samples) and by FIA-Chemiluminescence detection after acidification of the sample (de Jong et al., 2000). The result of this exercise showed a good agreement of dissolved Fe concentrations between these two fundamentally different techniques and is presented in detail elsewhere (de Jong et al., 2000).

Total dissolved iron concentrations were determined after UV-digestion, and labile concentrations before UV-digestion, except samples from the deep waters at station (St.) 10 which were analysed without UV-digestion but at a high concentration (50 μM) of NN (high-labile iron) after 2 min equilibration in the voltammetric cell prior to the measurement by CSV. The high-labile iron concentrations, and the mean ratio of $Fe_{UV}/Fe_{labile} = 1.54$ at St. 4, 8, 9 and 10, was used to obtain comparable numbers for the total dissolved iron concentrations for the deep waters at St. 10.

Iron complexing ligands were titrated with iron with detection of labile iron by CSV using ligand competition against the analytical ligand NN to evaluate the complex stability (Gledhill and van den Berg, 1994; Van den Berg, 1995; Boye et al., 2001). The titrations were at pH 8.0 using 0.01 M HEPPS pH buffer and 5 μM NN. Equilibration was overnight, and the bromate was added 3 min before the first voltammetric scan.

Fe(II) concentrations were calculated by difference between the iron measured before (= labile iron) and after (= labile Fe(III)) the addition of a specific-Fe(II) binding ligand (10 μM of 2,2-bipyridyl, Bp) to the filtered sample, using 20 μM of NN, 40 mM of bromate and 0.01 M HEPPS (Aldrich and van den Berg, 1998); the NN was added 30 min after the Bp addition. The detection limit was 0.1 nM Fe(II).

2.2.4. Calculation of the organic complexation of iron at thermodynamic equilibrium

Ligand concentrations (L) and conditional stability constants ($K'_{FeL} = [FeL]/([Fe^{3+}][L'])$) were calculated by linear least-squares regression of the titration data to the following equation (Van den Berg and Kramer, 1979; Ruzic, 1982; Van den Berg, 1982):

$$[Fe_{labile}]/[FeL] = [Fe_{labile}]/[L] + (\alpha_{Fe} + \alpha_{FeNN_3})/([L]K'_{FeL}). \quad (1)$$

Here $\log \alpha_{Fe} = \log([Fe']/[Fe^{3+}]) = 10$ (Hudson et al., 1992), where [Fe′] is the concentration of inorganic iron including all inorganic Fe(III) species, and $\log \alpha_{FeNN_3} = \log([Fe(III)NN_3]/[Fe^{3+}])$ which was calculated from $\log \alpha_{FeNN_3} = \log(\beta'_{FeNN_3}[NN]^3) = 12.5$ (using $\log \beta'_{FeNN_3} = 28.39$ (Gledhill and van den Berg, 1994)).

The relative standard deviation of repeated (5 ×) determinations of the ligand concentration was better than 10%, and better than 1% for the conditional stability constant.

The free metal ion concentration [Fe^{3+}], the inorganic metal concentration [Fe′], the concentration of organic metal complexes [FeL] were calculated assuming thermodynamic equilibrium, as described before (Boye et al., 2001).

3. Results

3.1. Sampling area hydrography

The northern part of the study area (St. 2) was characterized by deep vertical mixing (upper 150 m) associated with strong winds (Fig. 2). Between 37°N and 42°N, the surface waters of the southern stations were under the influence of the broad circulation scheme of the North Atlantic subtropical gyre. Along the 23°W meridian, the water column was characterized by a complex series of remnant mixed layers in the upper waters. The mixed layer occupied the upper 50 (St. 8) to 100 m (St. 6). Below this a pycnocline of ~10 m extent separated a deeper remnant mixed layer that reached down to ~150 m, which is the deepest winter-time mixed layer in this region (Measures et al., 1995). From approximatively 200 m, the base of the various mixed layers, to

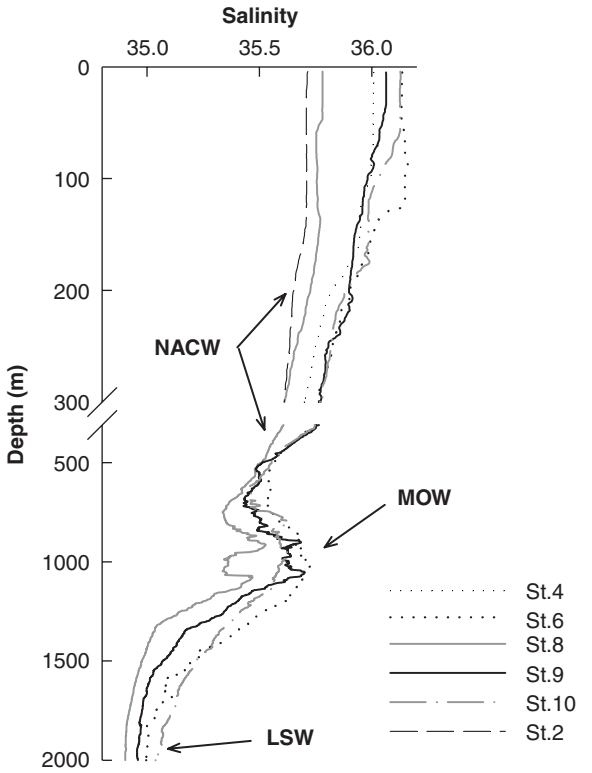

Fig. 2. The salinity in the water column at the 6 stations. Three well-characterized water-masses are indicated: NACW, North Atlantic Central Water; MOW, Mediterranean Outflow Water; LSW, Labrador Sea Water.

~900 m a linear T/S region revealed the presence of the North Atlantic Central Water (NACW), formed in the northeast Atlantic by deep winter-time convection. Underlying the NACW was the high-salinity Mediterranean Outflow Water (MOW) centred around 800–1100 m (Fig. 2). Its salinity signature was about 35.5 (St. 8) to 35.7 (St. 6) decreasing to the north. MOW represents a dilute form of the Mediterranean source water that exits at the Strait of Gibraltar as a mix of Levantine Intermediate Water and the underlying Western Mediterranean Deep Water, with a salinity of 38.44 (Measures and Edmond, 1988). Using this latter value and assuming that the MOW mixes with NACW with a mean salinity of 35.44 ± 0.07 (the value of the NACW salinity minimum above the MOW), then the average salinity of the MOW (35.65 ± 0.08) in the study area indicates a 14 fold dilution (7.1% original MOW and 92.9% NACW). Below the MOW a mix of North Atlantic Deep Water and Labrador Sea Water (LSW) is found.

3.1.1. Nitrate and chlorophyll-a (Chl-a)

Nitrate was depleted in the upper-mixed layer, except in the northern part of the area, at St. 8 which had residual levels of 3–4 μM nitrate (Fig. 3). Higher nitrate levels in the surface waters at St. 8 are in line with upwelling of nutrient-rich deep waters due to the influence of the more or less permanent frontal system (at about 42°N) associated with the northern side of the North Atlantic gyre (de Jong et al., 2000; Nolting et al., 2000). Nitrate concentrations in the surface waters slightly decreased over the 7-days sampling time from St. 6 to 10 (Fig. 3).

The nitrate concentrations increased with depth below the mixed layer (Fig. 3), converging to similar levels at all stations below the deepest winter mixed layer (~250 m), at concentrations between 8.7 and 19 μM NO_3.

Chl-*a* concentrations was between 0.5 and 1.3 $\mu g\,L^{-1}$ in the chlorophyll maximum. The southern part of the area (St. 6 and 10) was characterized by a sub-surface maximum of Chl-*a* at depths between ~40 and 70 m, whilst the northern part (St. 2, 4, 8, 9) showed a band of relatively uniform chlorophyll levels in the upper ~50–75 m of the water column except at St. 2 where the chlorophyll band extended to 150 m depth, probably resulting from wind-associated deep mixing (Fig. 3). Chl-*a* concentrations slightly decreased over 7 days (i.e. the sampling time between St. 6 and 10), as shown in Fig. 3. The chlorophyll concentration generally increased northward along the 23°W meridian and had highest levels at St. 8.

3.1.2. Major algal species composition

The large eukaryotes (>5 μm) dominated in terms of relative chlorophyll fluorescence biomass at all stations, except at St. 2 and 10 (data not shown). However, the large eukaryotes were numerically not the predominant species (see below). As a result, the cells' abundance pattern differs somewhat from the chl-*a* pattern (Figs. 3 and 4).

Cell numbers in the upper 50 m were greater at St. 4 [$(58 \pm 9) \times 10^3$ cells mL^{-1}, $n = 6$] and St. 8 [$(54 \pm 3) \times 10^3$ cells mL^{-1}, $n = 5$] than at the more southerly St. 9 and 10 (about 39×10^3 cells mL^{-1}) (Fig. 4). Over the 7-day sampling time between St. 6 and St. 10, phytoplankton cell numbers increased throughout the upper 50 m (St. 10), from a peak at greater depth at St. 6 (Fig. 4). This increase in cell numbers was mainly due to *Synechococcus*, which

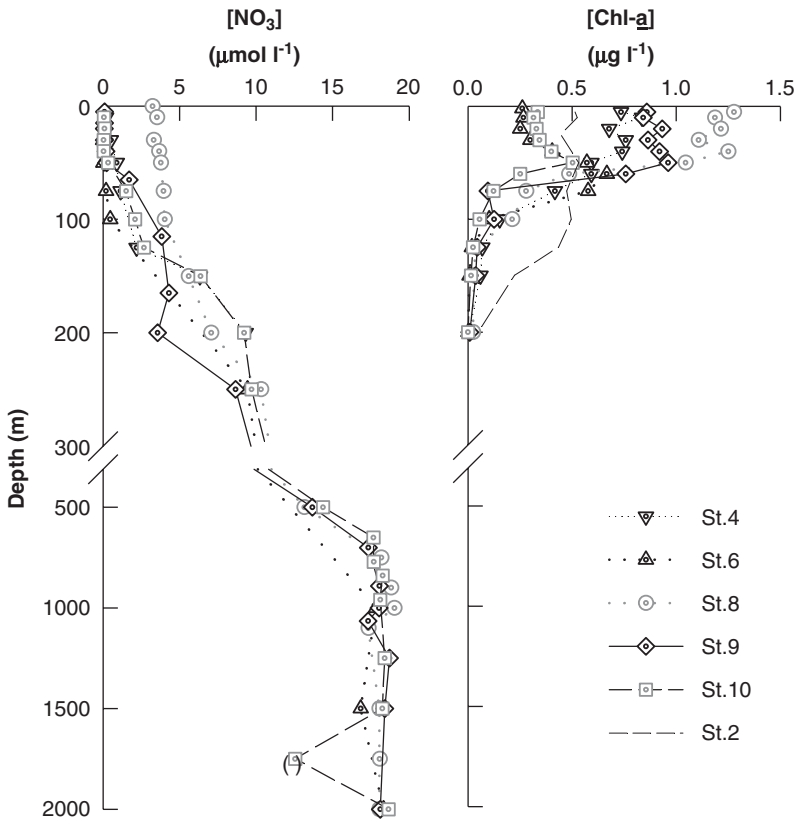

Fig. 3. Distribution of nitrate (NO_3) and chlorophyll-*a*, in the upper water column (0–200 m) for St. 2 and 4, and between 0 and 2000 for St. 6–10. No NO_3 data were available for St. 2.

dominated the cell numbers and contrasts with a decrease in chlorophyll over the same period.

Pico-phytoplankton (<2 μm) dominated numerically the phytoplankton community in the surface waters. Within this size class the photo-autotrophic cyanobacteria *Synechococcus* dominated at all stations (60–80% of total cells number) (Fig. 4), except at St. 4 and 8 where another pico-eukaryote co-occurred. In the southern part of the area, the phytoplankton composition changed during the 7-day sampling time between St. 6 and 10, mainly caused by increases in the relative abundance of *Synechococcus* (Fig. 4).

3.2. Metal speciation

3.2.1. Dissolved iron

The distribution of dissolved iron in the water column showed depletion (concentrations generally <1 nM, with a mean value of 0.79 ± 0.24 nM, $n = 30$) within the chlorophyll maximum, and higher concentrations in the deeper waters (below the nutricline, at ~500 m) of $\sim 1.4 \pm 0.1$ nM ($n = 26$); except at St. 2 where iron and Chl-*a* were uniformly distributed over the top 150 m because of the wind-associated deep mixing (Fig. 5; Table 1). The iron concentration in the MOW (1.44 ± 0.07 nM Fe, $n = 8$) was similar to that in the deeper waters, and ~1.6 × greater than in the winter-mixed layer (0.9 ± 0.3 nM). The calculated effect of dilution of MOW containing 2–3 nM Fe (Van den Berg, 1995) at a ratio of 1:14 with Atlantic deep water containing ~1.4 nM would be an increase of around 0.1 nM Fe if no iron is lost because of its low solubility. Our data does not have sufficient resolution demonstrate such a small increase in the iron concentration.

3.2.2. Organic iron complexing ligands

The concentration of the iron complexing ligands was 1.5–5 times greater than that of dissolved iron, and was between 1.2 and 3.5 nM in the upper water column (above the nutricline), and between 1.6 and 3.1 nM below the nutricline. Average concentrations

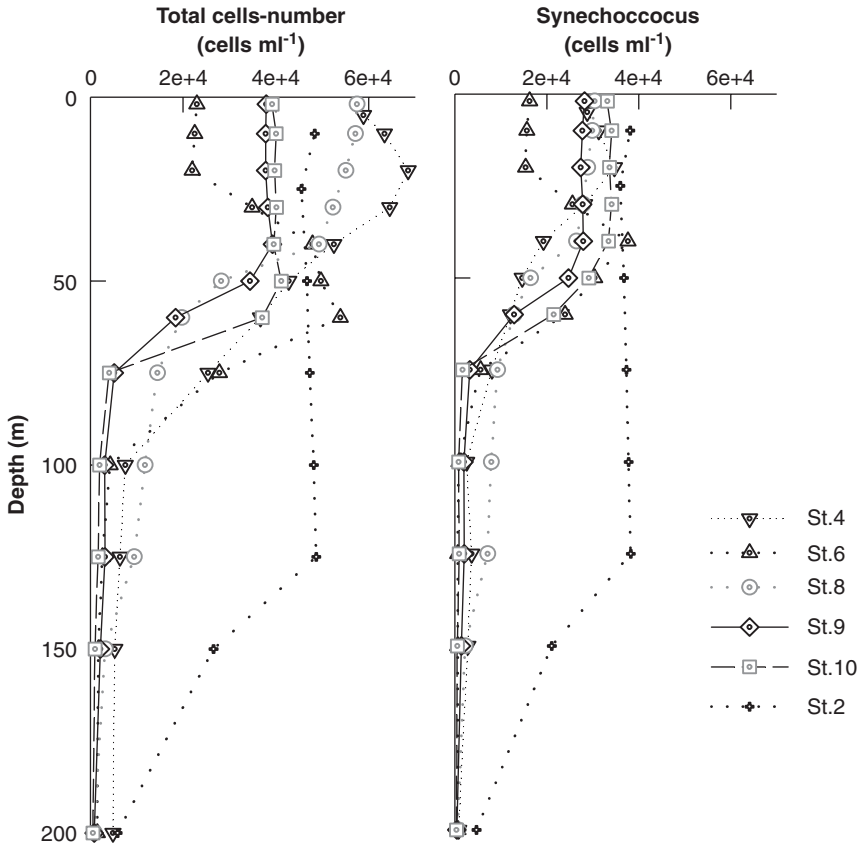

Fig. 4. Total cell-numbers (cell-density) and *Synechococcus* abundance in the upper water column (200 m) for the 6 stations.

of the ligands were greater at depth (3.0 ± 0.4 nM, $n = 45$) than within the Chl-*a* band (2.1 ± 0.5 nM, $n = 27$) (except at St. 4, see Fig. 5).

Vertical distributions of the ligand concentration generally showed a sub-surface maximum within or just below the Chl-*a* maximum (St. 4, 6, 8, 10), and a slight increase at depth below the nutricline (Fig. 5). This general trend was not followed at St. 2, where the ligand concentration was fairly constant (~2.3 nM) over the upper 150 m, consistent with the mixing of the upper water column by strong winds.

As for iron, no systematic north-southward trend was apparent for the ligand concentrations across the water masses, but a vertical gradient of its concentration was apparent. The ligand concentration in the MOW (2.7 ± 0.1 nM, $n = 8$) was 0.7 nM greater than in the winter mixed layer (2.0 ± 0.5 nM, $n = 43$). Below the MOW, ligand concentrations were generally slightly higher (2.4 ± 0.4 nM, $n = 11$) than those in the NACW (2.1 ± 0.2 nM, $n = 11$). The ligand concentration in the deep Mediterranean water is thought to be 6–8 nM (Van den Berg, 1995). 14-fold dilution of deep Mediterranean water with deep Atlantic water containing a ligand concentration of ~2 nM could cause a ligand concentration in the MOW about 0.5 nM greater than in the Atlantic water, which may well correspond to the increases seen in the MOW around 1000 m (Figs. 5 and 7).

The average complex stability ($\log K'_{FeL}$) across all stations was 20.9 ± 0.3 ($n = 73$), and was constant down the water column: 20.9 ± 0.4 ($n = 25$) within the Chl-*a* bands and in NACW, 21.0 ± 0.3 ($n = 8$) in the MOW and ~21 in the LSW.

3.2.3. Fe(II)

Fe(II) concentrations varied between below the detection limit (<0.1 nM) to 0.55 nM, and represented generally a small fraction (average 6%) but occasionally up to 50% of the dissolved iron concentration. The average concentrations of Fe(II) calculated for the water masses did not show a north–south trend. The vertical distribution of Fe(II) showed significant levels in the surface waters

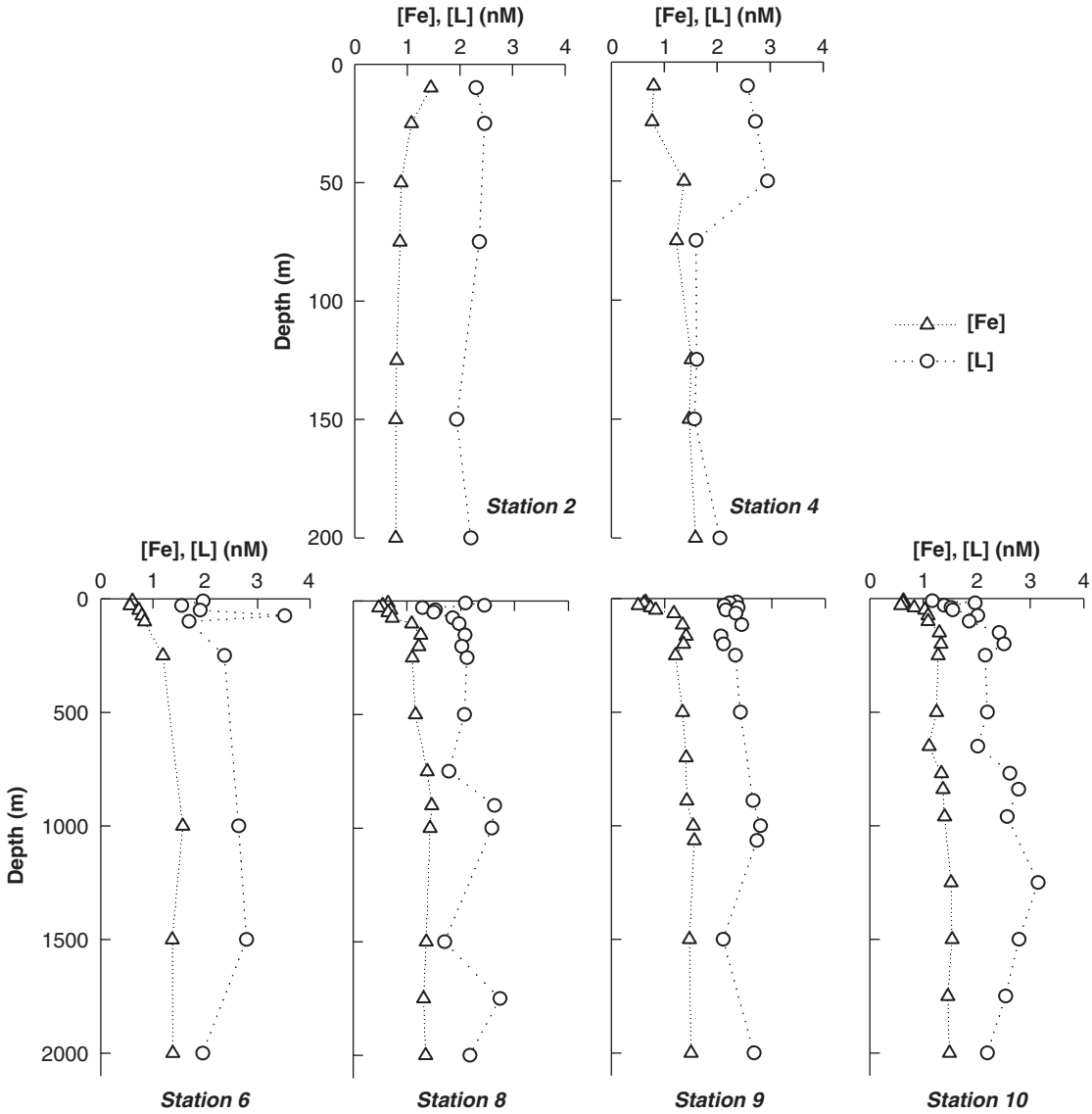

Fig. 5. Water column concentration of dissolved iron ([Fe]) and the dissolved iron-binding ligands ([*L*]) at the study stations (note: the depth-scale changes between St. 2–4 and the other stations).

(50 m depth) at St. 8 and 9 (Fig. 6), whilst Fe(II) was below the detection limit in the top 200 m at St. 10 (Fig. 6). The Fe(II) concentrations tended to increase with the Chl-*a* concentration, showing a maximum at and just below the Chl-*a* maximum (Figs. 6 and 3). In the deeper waters, Fe(II) was present at St. 8 (900 m), St. 9 (900 and 1065 m) and St. 10 (between 900 and 1500 m) at depths where the concentrations of dissolved iron and the organic ligands generally increased (Fig. 6). The vertical gradient of Fe(II) showed a factor 1.8–2.9 difference between its concentration in the upper winter mixed layer ($[\text{Fe(II)}] = 0.05 \pm 0.1$ nM, $n = 24$) and in the MOW ($[\text{Fe(II)}] = 0.1 \pm 0.14$ nM, $n = 8$) or below this in the LSW: $[\text{Fe(II)}] = 0.16 \pm 0.18$ nM ($n = 10$).

3.2.4. Iron speciation at thermodynamic equilibrium

The ligand concentrations were in excess of dissolved iron with an average concentration of 2.2 ± 0.5 nM ($n = 73$) for L compared to 1.1 ± 0.33 nM ($n = 73$) for Fe. Calculation of the chemical speciation of iron at thermodynamic equilibrium shows that dissolved iron was 98.5% organically bound throughout the water column

Table 1
The organic speciation of dissolved iron (<0.2 μm), showing dissolved iron (Fe), ligands (L), stability constant (K'), organic iron (FeL), inorganic iron calculated at thermodynamic equilibrium (Fe′), reduced iron (Fe(II)), and inorganic Fe(III) corrected for the concentration of Fe(II): $[Fe'_{cor}] = ([Fe]_{dissolved} - [Fe(II)])/[Fe]_{dissolved} \times [Fe']$

Station number and location	Depth (m)	$[Fe_d]$ (nM)	Fe(II) (nM)	$[L]$ (nM)	SD_L	Log K'	$SD_{\log K'}$	[FeL] (nM)	[Fe′] (pM)	$[Fe'_{cor}]$ (pM)
St. 2 45.23.5°N,	10	1.45	n.a.	2.31	0.44	20.97	0.04	1.43	17	—
10.37.50°W	25	1.08	n.a.	2.47	0.58	20.59	0.03	1.06	19	—
	50	0.88	n.a.	n.a.	—	n.a.	—	—	—	—
	75	0.86	n.a.	2.37	0.65	20.71	0.01	0.85	11	—
	125	0.80	n.a.	n.a.	—	n.a.	—	—	—	—
	150	0.78	n.a.	1.94	0.72	20.86	0.01	0.77	9	—
	200	0.78	n.a.	2.21	0.75	20.71	0.03	0.77	10	—
St. 4 40.30.05°N,	10	0.80	n.a.	2.57	0.72	20.55	0.05	0.79	12	—
17.47.52°W	25	0.77	n.a.	2.72	0.61	20.56	0.05	0.76	11	—
	50	1.37	n.a.	2.95	0.45	20.75	0.01	1.35	15	—
	75	1.23	n.a.	1.6	0.5	20.73	0.01	1.18	52	—
	125	1.51	n.a.	1.61	0.54	20.62	0.03	1.37	138	—
	150	1.47	n.a.	1.57	0.36	20.92	0.06	1.38	88	—
	200	1.59	n.a.	2.05	0.57	20.79	0.01	1.54	49	—
St. 6 37.28.9°N,	10	0.61	n.a.	1.96	0.34	22.25	1	0.61	0.3	—
22.58.70°W	30	0.56	n.a.	1.55	0.26	21.6	0.26	0.56	1.4	—
	50	0.73	n.a.	1.9	0.66	20.72	0.05	0.71	12	—
	75	0.79	n.a.	3.52	0.44	20.64	0	0.79	7	—
	100	0.84	n.a.	1.69	0.65	20.56	0.09	0.81	26	—
	250	1.19	n.a.	2.37	0.63	20.68	0.03	1.17	20	—
	1000	1.57	n.a.	2.64	0.53	20.36	0.01	1.52	58	—
	1500	1.37	n.a.	2.79	0.51	20.76	0.02	1.35	16	—
	2000	1.38	n.a.	1.95	0.58	20.72	0.02	1.34	42	—
St. 8 (surface)	10	0.65	0.07	2.09	0.48	20.75	0.03	0.64	8	7.02
42.35.82°N, 23.00.26°W	20	0.55	0.11	2.44	0.57	20.6	0.07	0.54	7	5.70
	30	0.48	0	1.29	0.48	21.12	0.05	0.48	4	4.48
	40	0.70	0.11	1.53	0.37	21.05	0.06	0.69	7	6.21
	50	0.65	0	1.5	0.38	21.05	0.08	0.65	7	6.74
	75	0.73	0.08	1.85	0.57	20.73	0.01	0.72	12	10.53
	100	1.09	0	1.97	0.49	20.79	0.02	1.07	19	19.41
	150	1.26	0.14	2.08	0.09	21.22	0.13	1.25	9	8.08
	200	1.22	0	2.02	0.39	21.11	0.11	1.20	12	11.47
St. 8 (deep) 42.34.18°N,	250	1.10	0	2.12	0.39	20.52	0.05	1.07	31	30.92
23.02.34°W	500	1.16	0	2.07	0.29	21.18	0.1	1.15	8	8.29
	750	1.38	0	1.78	0.22	20.98	0.05	1.35	33	32.56
	900	1.46	0.12	2.63	0.28	21.17	0.08	1.45	8	7.68
	1000	1.43	0	2.58	0.32	21.25	0.1	1.43	7	6.97
	1500	1.36	0	1.7	0.2	21.44	0.18	1.35	14	14.00
	1750	1.31	0	2.73	0.7	20.72	0	1.29	17	17.15
	2000	1.35	0.08	2.17	0.31	21.11	0.09	1.34	12	11.75
St. 9 (surface)	15	0.64	0	2.34	0.39	20.93	0.12	0.63	4	4.36
40.00.17°N, 23.00.01°W	20	0.61	0	2.21	0.55	20.6	0.05	0.60	9	9.46
	30	0.50	0.26	2.11	0.32	20.85	0	0.50	4	2.10
	40	0.73	0.22	2.37	0.48	20.7	0.02	0.73	9	6.15
	50	0.83	0	2.14	0.37	21.14	0.02	0.83	5	4.56
	65	1.17	0.3	2.33	0.72	20.87	0.03	1.16	13	9.87
	115	1.33	0	2.44	0.21	21.1	0.05	1.32	9	9.42
	165	1.40	0	2.05	0.6	20.68	0.03	1.36	41	41.01
	200	1.35	0	2.1	0.22	21.26	0.11	1.34	10	9.74
	250	1.20	0	2.32	0.45	21.09	0.1	1.19	9	8.52

Table 1 (*continued*)

Station number and location	Depth (m)	[Fe_d] (nM)	Fe(II) (nM)	[L] (nM)	SD_L	Log K'	$SD_{\log K'}$	[FeL] (nM)	[Fe′] (pM)	[Fe'_{cor}] (pM)
St. 9 (deep) 40.00.31°N, 22.59.84°W	500	1.33	0	2.41	0.24	20.85	0.02	1.31	17	16.79
	700	1.40	0	n.a.	—	n.a.	—	—	—	—
	890	1.41	0.12	2.65	0.14	21.05	0.08	1.40	10	9.13
	1000	1.53	0	2.79	0.44	20.89	0.03	1.51	15	15.28
	1065	1.55	0.12	2.72	0.44	20.91	0.03	1.54	16	14.72
	1250	—	0	n.a.	—	n.a.	—	—	—	—
	1500	1.46	0.13	2.09	0.48	21.2	0.08	1.44	14	12.81
	2000	1.49	0.19	2.67	0.48	21.17	0.11	1.48	8	7.37
St. 10 (surface) 37.00.54°N, 22.59.55°W	10	0.63	0	1.17	0.21	21.03	0.05	0.62	11	10.50
	20	0.62	0	1.97	0.58	20.78	0.02	0.61	7	7.50
	30	0.58	0	1.39	0.14	21.21	0.08	0.58	4	4.41
	40	0.83	0	1.52	0.58	20.7	0.03	0.81	23	22.89
	50	1.03	0	1.55	0.32	20.97	0.02	1.01	20	19.83
	75	1.09	0	2.02	0.45	20.78	0	1.07	19	18.69
	100	1.09	0	1.86	0.65	20.57	0.07	1.05	35	35.09
	150	1.30	0	2.42	0.45	21	0.06	1.29	11	11.41
	200	1.33	0	2.51	0.6	20.93	0.05	1.32	13	12.99
St. 10 (deep) 37.00.10°N, 23.00.15°W	250	1.28[a]	0	2.16	0.22	21.05	0.05	1.27	13	12.65
	500	1.25[a]	0	2.2	0.32	20.87	0.03	1.23	17	17.19
	650	1.11[a]	0	2.02	0.51	20.74	0.01	1.09	21	21.27
	770	1.34[a]	0	2.62	0.31	21.09	0.06	1.33	8	8.40
	840	1.37[a]	0	2.78	0.71	20.98	0.05	1.36	10	10.03
	960	1.40[a]	0.42	2.57	0.37	21.14	0.09	1.39	9	5.99
	1250	1.52[a]	0.32	3.15	0.69	20.68	0.01	1.50	19	15.02
	1500	1.54[a]	0.55	2.79	0.48	21.03	0.25	1.53	11	7.27
	1750	1.46[a]	0	2.54	0.39	20.91	0.16	1.44	16	16.20
	2000	1.49[a]	0.3	2.2	0.21	21.17	0.07	1.48	14	11.01

Note: n.a. means not analyzed, — indicates determination not possible.

[a]Calculated using $Fe_{UV}/Fe_{labile} = 1.54$ (e.g. the slope of $Fe_{UV} = f(Fe_{labile})$ using data from St. 4, 8, 9 and 10).

(not considering Fe(II) for now), similar to that observed in other oceanic waters, such as the North Pacific (Rue and Bruland, 1995), the Equatorial Pacific (Rue and Bruland, 1997), the North Atlantic (Gledhill and van den Berg, 1994; Wu and Luther, 1995; Witter and Luther, 1998), the South and Equatorial Atlantic (Powell and Donat, 2001), the Mediterranean Sea (Van den Berg, 1995) and the Southern Ocean (Boye et al., 2001; Nolting et al., 1998).

The average α-coefficient for organic complexation of iron was (log value) 12.3 ± 0.3 ($n = 73$). The average concentration of inorganic iron (Fe′) at thermodynamic equilibrium was 18 (± 20) pM ($n = 73$), and its fraction of dissolved iron was 1.5 (± 1.3)%.

The vertical profiles of inorganic iron (Table 1) showed some variability with depth, and generally the concentrations of inorganic iron were lower in the Chl-*a* layer than at greater depth. A sub-surface maximum occurred at depths of 100–160 m, just on or below the nutricline, which may be evidence of regeneration.

4. Discussion

4.1. The distribution of dissolved iron (0–2000 m)

All stations (except the short St. 2) showed lower upper water column (top 250 m) concentrations than deeper water levels (Fig. 5), in line with uptake by phytoplankton and regeneration at depth. Most stations also had a slightly higher iron concentration in the sample(s) nearest the surface at 10–20 m depth (Table 1), indicative of aeolian deposition which is the dominant process for iron input in this region (Duce and Tindale, 1991; Visser et al., 2003). In the thermocline, below 250 m, the concentration of dissolved iron increased, similar to that of nitrate. The increase in the iron concentration was

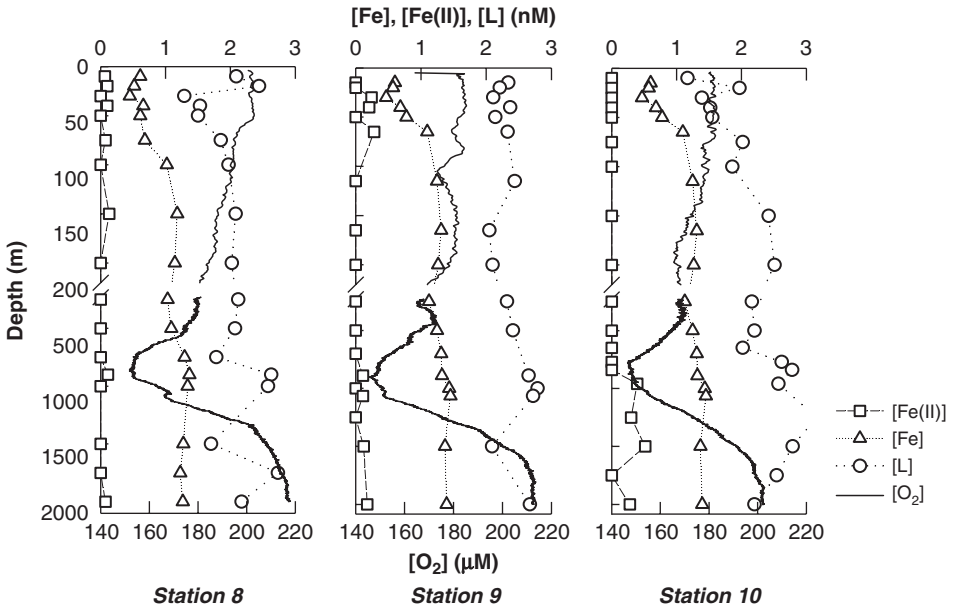

Fig. 6. Comparison of the distribution of dissolved iron (Fe), reduced iron (Fe(II)), the Fe(III)-binding organic ligand (L) and dissolved oxygen (O_2) in the water column of St. 8–10.

positively correlated to that of nitrate ($[NO_3]_{\mu M} = 20[DFe]_{nM} - 11$, $r^2 = 0.60$, $n = 30$) at all deep water stations (6, 8, 9, and 10), consistent with the remineralization of biogenic particles at depth, releasing iron and nutrients at a relatively constant ratio (Johnson et al., 1997).

Previous studies of the northeast Atlantic Ocean, either north (Martin et al., 1993; Laës et al., 2003) or south (Landing et al., 1995; Wu et al., 2001) of our study area, generally found lower iron concentrations in the water column (0.3–0.8 nM less) than reported here. The relatively elevated dissolved iron concentrations recorded in our survey could be due to a systematic offset in our data or to input from a Saharan dust storm that crossed the area at the beginning of our cruise. Evidence of the dust plumes can be seen on SeaWIFS satellite images from 4–17 March 1998. The dust outbreak that started at the beginning of March was an extension of an earlier period of dust pulses in January–February 1998 (Torres-Padrón et al., 2002) classified as the highest dust outbreak activity in the Canary Island region since 1985 (Pérez-Marrero et al., 2002). Similar elevated dissolved iron concentrations (~1.04 nM in the surface mixed-layer and ~1.65 nM at depths below 250 m) were detected by a different analytical method (FIA-chemiluminescence), and high dissolved aluminium concentrations (~16 nM in the surface mixed-layer to ~24 nM in the MOW), which can be used as a proxy of atmospheric dust input, were recorded in these waters during the same cruise (de Jong et al., 2000; de Jong et al., submitted). Several observations have shown that atmospheric dust deposition may episodically and locally increase the Fe concentration in oceanic surface waters (Bruland et al., 1994; Kremling and Streu, 1993; Sarthou et al., 2003; Lenes et al., 2001). However it was not expected that dust deposition would leave as high iron levels in its wake as recorded in our survey to be exported to the deeper waters, since the solubility of iron in atmospheric particles is thought to be extremely low (Jickells and Spokes, 2001) and the residence time of iron in surface seawater rather short (Jickells, 1999; de Baar and de Jong, 2001). For this reason we do not wish to exclude the possibility that later data will demonstrate that our iron concentrations are too high.

The detected ligand concentrations (see below) were always much greater than the iron concentrations, so the conclusions of this work are not affected by a possible systematic error in the iron concentrations at some of the stations. However, the absolute ligand concentrations would be overestimated by the same amount (0.3–0.8 nM) as the iron concentrations.

4.2. Distribution of Fe-binding ligands in the water column (0–2000 m)

The ligand concentrations found in this study were generally lower than those reported previously for the North Atlantic Ocean (Gledhill and van den Berg, 1994; Wu and Luther, 1995; Witter and Luther, 1998), and also the conditional stability constants (average $\log K$ value of 20.9) were generally lower, and also lower than $\log K$ values (around 22–24) reported for the Equatorial and South Atlantic (Powell and Donat, 2001). It is not clear whether this systematic difference is due to abundance of different ligands or due to different methods of calculation as some of the literature data is based on Fe′ concentrations and ours on Fe^{3+}.

The vertical distribution of the ligands showed systematic variations with depth, indicative of processes of production and removal. Several stations (2, 4 and 10) showed a near-surface depletion of the ligands, suggesting photochemical breakdown of the ligands. The possibility of this process has been reported before for complexing ligands of iron (Van den Berg, 1995; Rue and Bruland, 1997) and copper (Moffett et al., 1990). In association with the photochemical breakdown of the organic ligands it is possible that the iron is reduced and released as Fe(II) by microorganisms (Rue and Bruland, 1997), which, however, is not apparent in the profiles of Fe(II) at St. 8 and 9 (Fig. 6). The time scale of photochemical Fe(III) reduction and subsequent oxidation is much shorter than that for photochemical breakdown of the ligands, so it is quite likely that the signal of photochemical breakdown is apparent from lower ligand concentrations but not in the presence or absence of Fe(II).

At some stations (4 and 10) the ligand concentration was greater within the chlorophyll layer than below. One ligand concentration, at 75 m at St. 6, stood out as being very high, and was located just below the *Synechococcus* cell-number maximum. Ligand concentrations were almost as high at St. 4, also peaking below the *Synechococcus* layer, which suggests that this cyanobacterium could be an important source of the ligands. For instance, the high-integrated concentration of the ligands in the chlorophyll layer at St. 4 (Fig. 5) coincides with the highest *Synechococcus* cell-number found during this cruise (Fig. 4). However, no simple relation is apparent between the ligands and the chlorophyll (or the cell number) concentration, as linear regressions gave positive (St. 4) as well as negative (St. 8, 10) fits. This suggests that ligand removal processes were superimposed on the production processes, causing systematic variations during the procession of phytoplankton development. For instance, the increase in *Synechococcus* sp. abundance and the dissolved iron concentration in surface waters from St. 6 to 10 was not followed by an increase in the ligand concentration. Cyanobacteria are thought to rely on siderophore–Fe complexes to obtain iron (Granger and Price, 1999). It is possible that ligands were produced after the apparent iron input, and removed again (presumably complexed with iron) as a result of uptake by the growing *Synechococcus* sp., if the ligands were siderophore-type ligands. The very high ligand concentration (3.5 nM) at 75 m at St. 6 has disappeared at St. 10 and the surface ligand concentrations decreased (from 2.12 ± 0.8 nM, $n = 5$, at St. 6; to 1.52 ± 0.29, $n = 5$, at St. 10). Based on that decrease, the removal rate of the ligands by *Synechococcus* sp. would be equivalent to $\sim 1.22 \times 10^{-8}$ nmol cell^{-1} d^{-1}, by Δ[cells mL^{-1}]$\sim 7 \times 10^{3}$ as detected over the 7 days sampling time between St. 6 and 10.

The nature of the organic ligands is still uncertain in oceanic waters. The complex stability of the ligands found in this study (average $\log K'_{FeL} = 20.9$) is less than that for siderophores which have $\log K$ values nearer 23 (Rue and Bruland, 1995, 1997), suggesting that these ligands might be chemically different. However this difference does not rule out the possibility that both classes of ligands were siderophores-type chelators. Indeed autotrophic bacteria, such as *Synechococcus* sp. and *Prochlorococcus* sp., as well as heterotrophic bacteria, are extremely abundant in the surface waters of the equatorial Pacific Ocean (Chavez et al., 1991; Kirchman et al., 1995), while *Synechococcus* dominated the pico-assemblage in the surface waters of the northeastern Atlantic Ocean. Since both cyanobacteria and heterotrophic bacteria are known to be capable of producing siderophores (Wilhelm and Trick, 1994, 1995; Reid et al., 1993), it can be expected that different types of siderophores are produced by the different prokaryote assemblages of the Pacific and of the Atlantic. Furthermore it is unlikely that the ligands were degradation organic products, such porphyrins (Rue and Bruland, 1995, 1997), released during grazing (Hutchins and Bruland, 1994) or cell lysis (Rue and Bruland, 1997). Indeed the general decrease in the ligands concentration while the pico-assemblage decreased over

the 7 days between St. 6 and 10, probably due to nutrients limitation, did not fit with ligands being degradation products.

The deep-water ligand concentrations were generally greater than within the euphotic layer, suggesting that the ligands are either released from sinking biogenic particles, or by bacteria living in the deep waters. The constant complex stability throughout the water column suggests that the ligands must have been of a similar composition, but it is possible that a method with better resolution would discover systematic differences.

Highest ligand concentrations in the deep waters were found within the waters associated with MOW, (Fig. 2). Their complex stabilities ($\log K'_{FeL} \sim 21.0$) are in the range that was observed before in the Mediterranean ($\log K'_{FeL} = 19.8$–21; Van den Berg, 1995), indicating that the ligands are similar. The ligand concentrations within the MOW (2–2.5 nM) were lower than in the Mediterranean (6–8 nM) (Van den Berg, 1995), which is to be expected because of dilution of the Mediterranean water on its journey northward into the Atlantic Ocean. If the ligands observed in the MOW are in part the same as those produced within the Mediterranean Sea, that would mean that these ligands behaved conservatively. On the other hand, it is also possible that a higher remineralization rate associated with the oxygen minimum of the MOW (Fig. 6) causes the increase of the ligand concentration at those depths.

The comparison of the ligand concentration in deep waters below the MOW (from ~1000 to 2000 m) from the North Atlantic (~2.4 nM, this study) to equatorial and South Atlantic waters (~1.8 nM, Powell and Donat, 2001) and to the Atlantic sector of the Southern Ocean (~0.7 nM, Boye et al., 2001) indicates a southward decrease. This horizontal gradient contrasts with the fairly constant vertical distribution of the ligand in deep waters. This indicates that while sources and sinks of the ligand may be balanced in deep waters, the residence time may be shorter than the time scale of water-mass circulation. Only one chemical ligand group has been detected in this study in the deep waters, but it is possible that more than one class is present. As pointed out previously (Boye et al., 2001) it is possible that another ligand with a background concentration of ~0.7 nM (such as found in the deep waters of the Southern Ocean) occurs in the deep Atlantic waters, where it was masked by the slightly greater iron concentration and the presence of a ligand at higher concentration. In this case the weaker ligand group with the relatively higher concentration detected in the deep Atlantic would be more chemically reactive than the stronger ligand co-occuring at a lower concentration, and was lost first during the deep water masses circulation. Thus only the stronger ligand class would be detected in the Southern Ocean. This hypothesis would also fit with colloidal- (weak) ligand aggregation (Wu et al., 2001) controlling the deep-water ligand concentration-gradient between the ocean basins, hence the inter-ocean deep Fe fractionation.

Interestingly the concentration of dissolved iron in the water column of the Atlantic is greater than its solubility as inorganic iron (0.1–0.2 nM at pH 8.1; Millero, 1998; Wu et al., 2001), which should lead to iron precipitation especially in the more highly iron-supersaturated deep waters. It is likely that the complexation with organic ligands (~98%) maintains the dissolved iron at levels greater than its solubility. Therefore the production of organic ligands under the Saharan dust belt and the organic complexation favoured the large atmospheric input of iron to the NE-Atlantic to be kept elevated in these waters, hence controlling the potentially available iron reserves.

4.3. Vertical distribution of Fe(II) species

Fe(II) was present in the upper water column (up to 0.3 nM) and occasionally at greater depths especially in waters of predominantly Mediterranean origin (up to 0.55 nM), representing 0–50% of the dissolved iron concentration. These levels compare with concentrations of 0.2–1.2 nM Fe(II) (20–60% of the reactive-Fe concentration) in waters from the North Sea (Gledhill and van den Berg, 1995), of 0.12–0.53 nM Fe(II) in the upper 100 m depths of the equatorial Pacific (O'Sullivan et al., 1991) and of 0.16–0.86 nM Fe(II) in surface waters of a transect in the northeast Atlantic through the English Channel (not considering the highest levels in nearshore waters of up to 1.8 nM; Boye et al., 2003).

The half-life of Fe(II) in oxygenated sea water is thought to be between 2 and 70 min (Millero et al., 1987; Zhuang et al., 1995). In surface oxygenated seawater Fe(II) should then be rapidly oxidised to Fe(III) and could precipitate as hydrous ferric oxide colloids or be complexed by ligands (King et al., 1993). The presence of significant concentrations of

Fe(II) in surface waters therefore suggests that either Fe(II) is continuously produced, or it is stabilised. Processes that produce Fe(II) in the surface waters include photochemical reduction (e.g. Fe–organic complexes or inorganic oxyhydroxides; Waite et al., 1995; Voelker and Sedlak, 1995; Kuma et al., 1992), enzymatic reduction (e.g. extra or intra-cellulare enzymes; Barbeau et al., 1996; Hutchins et al., 1993; Maldonado and Price, 2000), chemical reduction of Fe(III) by electron exchanges with organic chelators (e.g. tannic acid; Rich and Morel, 1990) and reduction within microenvironments (e.g. grazers; Barbeau et al., 1996).

At St. 8 and 9 Fe(II) was present at and just below the Chl-*a* maximum and within the cell-abundance maximum, indicating a link between reduced iron and biological or microbial activity. Previous work has shown that Fe(II) is present throughout the mixed layer in the equatorial Pacific, with maxima near the surface and at depths with higher Chl-*a* concentration (O'Sullivan et al., 1991). Our study did not show a simple correlation between Fe(II) concentrations and the Chl-*a* content (or cell-abundance), suggesting that several processes of production and removal of Fe(II) may have been at work through the upper water column, as for the organic ligand and for dissolved iron. Possible processes of Fe(II) removal are chemical oxidation (Millero et al., 1987; Millero and Sotolongo, 1989; Kuma et al., 1996) and biological uptake (Jones et al., 1987). Fe(II) maxima in the euphotic layer were at nearly the same depth as maxima in the concentration of the organic Fe-binding ligand and of the depletion of dissolved iron at St. 8 and 9, while Fe(II) was not detectable in the upper water column at St. 10 (Fig. 6). This observation, coupled with the decrease of the organic ligand concentration at St. 10, may suggest a link between the production of Fe(II) species, the production of the organic ligand and the increase in cell numbers. It has been proposed for instance that the biota (bacteria or phytoplankton) may release ligands or reductants by exudation or as a by-product of biodegradation, which can enhance the reduction of iron (Sulzberger et al., 1989). Kuma et al. (1992) explained high concentrations of Fe(II) (20–40 nM) in oxic surface waters during a spring bloom by the photoreduction of Fe(III) in the presence of hydrocarboxylic acids, which were possibly released by phytoplankton during the spring bloom.

Fe(II) was also present in deep waters at St. 8, 9 and 10, within or just below the MOW. The presence of detectable Fe(II) levels at these depths is also associated with the increase of organic ligand concentrations. Interestingly the increase of Fe(II) and organic ligand concentrations within the MOW is associated with a decrease of the oxygen content (Fig. 6) which makes sense if iron is reduced generally as a result of reductive processes (organic matter breakdown) which were predominant at this depth. Oxygen was not fully depleted, and the persistence of Fe(II) in the presence of the dissolved oxygen could suggest that Fe(II) is possibly stabilized for instance by organic complexation (Santana-Castiano et al., 2000) or is oxidized very slowly because of stabilisation by the lower temperature at depth (Millero and Sotolongo, 1989; Millero et al., 1987).

4.4. Fe-bioavailability

There is still uncertainty about which form(s) of iron (organically complexed Fe(III), inorganic Fe(III), or Fe(II)) is bioavailable. Recent work indicates that the bioavailable iron may well be inorganic Fe(III) (Maldonado and Price, 2000) taken up in a reductive process. Counter intuitively the concentration of such Fe(III) can be enhanced by siderophores (Kuma et al., 2000), facilitating photochemical reduction of Fe(III) to transient Fe(II), with a subsequent re-oxidation to fresh Fe(III). In this study, total dissolved iron averaged 0.79 nM (± 0.24, $n = 30$) in the Chl-*a* layer of all stations; the iron was 99% organically complexed, leaving a *calculated* inorganic Fe(III) concentration of 10.4 ± 6 pM ($n = 26$) (disregarding the smallest and highest outliers). At the same time the *measured* concentration of Fe(II) averaged 70 ± 100 pM ($n = 16$). The presence of Fe(II) shows that these waters are not at thermodynamic equilibrium. The concentration of Fe(II) was greater than that of inorganic Fe(III), indicating that this transient Fe(II) greatly changes the chemical speciation of iron. The concentrations of Fe′ (inorganic Fe(III)) are shown in Table 1 with and without correction for the presence of Fe(II): it can be seen that the concentrations of Fe′ are lowered by 0–50% by correcting for Fe(II). The concentration of Fe(III) was well above the half saturation value ($K\mu_{Fe(III)}$) of 1.39 pM as reported recently for *Synechococcus* (Timmermans et al., 2005), making it very unlikely that this species is Fe-limited in these

waters. Furthermore, assuming that both inorganic Fe(III) and Fe(II) are equally bioavailable, and more so than organically bound Fe, the transient formation of Fe(II) would have increased the amount of bioavailable Fe by a factor of 10.

The decrease in dissolved iron within the Chl-*a* maximum (Fig. 6) indicates that the organic iron was (directly or indirectly) bioavailable. The organic Fe-uptake rate of *Synechococcus* sp. was thus estimated to be 1.22×10^{-17} mol Fe cell^{-1} d^{-1} during this study (assuming that the organic iron uptake rate is similar to that of the ligands estimated for St. 6 and 10, see above). This estimate is 5–40 × lower than the Fe-uptake of the coastal *Synechococcus PCC7002* (6.4×10^{-17} mol Fe cell^{-1} d^{-1} in absence of siderophores, and 48×10^{-17} mol cell^{-1} d^{-1} in presence of siderophores; re-calculated from Trick and Wilhelm, 1995), in agreement with an expected higher iron requirement of coastal species compared to their pelagic counterparts (Brand et al., 1983; Brand, 1991). Normalized to cell volume (using a cell volume of 2 μm^3, Trick and Wilhelm, 1995), the uptake rate of organic iron by *Synechococcus* sp. here is about 6 mmol Fe (liter cell volume)$^{-1}$ d^{-1}. This is in the range of the Fe-uptake rate of the coastal diatom *Thalassiosira weissflogii* (~6.5 mmol Fe (liter cell volume)$^{-1}$ d^{-1}; Hudson and Morel, 1990), but it is 7–20 × higher than the uptake rates of the oceanic diatom *Thalassiosira oceanica* at 0.5–0.8 mmol Fe (liter cell volume)$^{-1}$ d^{-1} (Sunda and Huntsman, 1995) and of the oceanic coccolithophore *Emiliania huxleyi* at 0.3–0.5 mmol Fe (liter cell volume)$^{-1}$ d^{-1} (Sunda and Huntsman, 1995). Compared to the standing stock of inorganic iron (10.4 pM in average) and of organic iron (770 pM) found in the North Atlantic, the estimated uptake rate of 1.22×10^{-2} fmol Fe cell^{-1} d^{-1} would suggest that *Synechococcus* sp. would not be limited by iron in the North Atlantic either by inorganic or organic Fe. This finding is in line with that observed in cultures using oceanic *Synechococcus* sp. isolated from the surface waters of the Sargasso Sea (Brand et al., 1983), which demonstrated that cyanobacteria were limited only at iron (added as FeEDTA) below 10^{-8} M (Brand et al., 1983), i.e. below ~8 pM inorganic iron (using $\log K'_{\mathrm{FeEDTA}} = 24.3$, Gerringa et al., 2000).

Acknowledgements

We thank the captain and crew of the Dutch research vessel *Pelagia*. Nutrient data are from Jan van Ooijen (NIOZ), CTD measurements were made by R. Groenewegen (NIOZ), and chlorophyll-*a* analysis by M. Davey (MBA). G.W. Raay (NIOZ) has contributed to the phytoplankton composition data. We much appreciate comments on the manuscript by three anonymous referees. This investigation was supported by the MERLIM project of the European Union (MAS3-CT95-0005).

References

Aldrich, A.P., van den Berg, C.M.G., 1998. Determination of iron and its redox speciation in seawater using cathodic stripping voltammetry. Electroanalysis 10 (6), 369–373.

Barbeau, K., Moffett, J.W., Caron, D.A., Croot, P.L., Erdner, D.L., 1996. Role of protozoan grazing in relieving iron limitation of phytoplankton. Nature 380, 61–64.

Behrenfeld, M.J., Kolber, Z.S., 1999. Widespread iron limitation of phytoplankton in the South Pacific Ocean. Science 283, 840–843.

Blain, S., Guieu, C., Claustre, H., Leblanc, K., Moutin, T., Quéguiner, B., Ras, J., Sarthou, G., 2004. Availability of iron and major nutrients for phytoplankton in the north-east Atlantic Ocean. Limnology and Oceanography 49 (6), 2095–2104.

Boye, M., van den Berg, C.M.G., de Jong, J.T.M., Leach, H., Croot, P., de Baar, H.J.W., 2001. Organic complexation of iron in the Southern Ocean. Deep-Sea Research I 48, 1477–1497.

Boye, M., Aldrich, A.P., van den Berg, C.M.G., de Jong, J.T.M., Veldhuis, M., de Baar, H.J.W., 2003. Horizontal gradient of the chemical speciation of iron in surface waters of the northeast Atlantic Ocean. Marine Chemistry 80, 129–143.

Brand, L.E., 1991. Minimum iron requirements of marine phytoplankton and the implications for the biogeochemical control of new production. Limnology and Oceanography 36, 1756–1771.

Brand, L.E., Sunda, W.G., Guillard, R.R.L., 1983. Limitation of marine-phytoplankton reproductive rates by zinc, manganese, and iron. Limnology and Oceanography 28 (6), 1182–1198.

Bruland, K.W., Orians, K.J., Cowen, J.P., 1994. Reactive trace elements in the stratified central North Pacific. Geochimica et Cosmochimica Acta 58, 3171–3182.

Chavez, F.P., Buck, K.R., Coale, K.H., Martin, J.H., DiTullio, G.R., Welshmeyer, N.A., Jacobson, A.C., Barber, R.T., 1991. Growth rates, grazing, sinking and iron limitation of equatorial Pacific phytoplankton. Limnology and Oceanography 36, 1816–1833.

Coale, K.H., Johnson, K.S., Fitzwater, S.E., Gordon, R.M., Tanner, S., Chavez, F.P., Ferioli, L., Sakamoto, C., Rogers, P.F., Millero, F., Steinberg, P., Nightingale, P., Cooper, D., Cochlan, W.P., Landry, M.R., Constantinou, J., Rollwagen, G., Trasvina, A., Kudela, R., 1996. A massive phytoplankton bloom induced by an ecosystem-scale iron fertilization experiment in the equatorial Pacific Ocean. Nature 383, 495–501.

de Baar, H.J.W., de Jong, J.T.M., 2001. Distributions, sources and sinks of iron in seawater. In: Turner, D., Hunter, K. (Eds.), The Biogeochemistry of Iron in Seawater, IUPAC Book Series on Analytical and Physical Chemistry of

Environmental Systems, vol. 7. Wiley, Chichester, pp. 123–253.

de Jong, J.T.M., Boye, M., Schoemann, V.F., Nolting, R.F., de Baar, H.J.W., 2000. Shipboard techniques based on flow injection analysis for measuring dissolved Fe, Mn and Al in seawater. Journal of Environmental Monitoring 2, 496–502.

de Jong, J.T.M., Boye, M., Timmermans, K.R., Veldhuis, M.J.W., Nolting, R.F., van den Berg, C.M.G., de Baar, H.J.W., submitted. Input of iron, aluminium and manganese to the surface mixed layer of the Northeast Atlantic Ocean and the European continental shelf waters. Deep-Sea Research I, submitted for publication.

DiTullio, G.R., Hutchins, D.A., Bruland, K.W., 1993. Interaction of iron and major nutrients controls phytoplankton growth and species composition in the tropical North Pacific Ocean. Limnology and Oceanography 38 (3), 495–508.

Duce, R.A., Tindale, N.W., 1991. Atmospheric transport of iron and its deposition in the ocean. Limnology and Oceanography 36, 1715–1726.

Gerringa, L.J.A., de Baar, H.J.W., Timmermans, K.R., 2000. A comparison of iron limitation of phytoplankton in natural oceanic waters and laboratory media conditioned with EDTA. Marine Chemistry 68, 335–346.

Gledhill, M., van den Berg, C.M.G., 1994. Determination of complexation of Fe(III) with natural organic complexing ligands in sea water using cathodic stripping voltammetry. Marine Chemistry 47, 41–54.

Gledhill, M., van den Berg, C.M.G., 1995. Measurement of the redox speciation of iron in seawater by catalytic cathodic stripping voltammetry. Marine Chemistry 50, 51–61.

Granger, J., Price, N.M., 1999. The importance of siderophores in iron nutrition of heterotrophic marine bacteria. Limnology and Oceanography 44, 541–555.

Hudson, R.J.M., Morel, F.M.M., 1990. Iron transport in marine phytoplankton: kinetics of cellular and medium coordination reactions. Limnology and Oceanography 35, 1002–1020.

Hudson, R.J.M., Covault, D.T., Morel, F.M.M., 1992. Investigations of iron coordination and redox reactions in seawater using 59Fe radiometry and ion-pair solvent extraction of amphiphilic iron complexes. Marine Chemistry 38, 209–235.

Hutchins, D.A., Bruland, K.W., 1994. Grazer-mediated regeneration and assimilation of Fe, Zn and Mn from planktonic prey. Marine Ecology-Progress Series 110, 259–269.

Hutchins, D.A., DiTullio, G.R., Bruland, K.W., 1993. Iron and regenerated production—evidence for biological iron recycling in 2 marine environments. Limnology and Oceanography 38 (6), 1242–1255.

Hutchins, D.A., Witter, A.E., Butler, A., Luther III, G.W., 1999. Competition among marine phytoplankton for different chelated iron species. Nature 400, 858–861.

Jickells, T.D., 1999. The inputs of dust derived elements to the Sargasso Sea: a synthesis. Marine Chemistry 68, 5–14.

Jickells, T.D., Spokes, L.J., 2001. Atmospheric iron inputs to the oceans. In: Turner, D.R., Hunter, K.A. (Eds.), The Biogeochemistry of Iron in Seawater. SCOR-IUPAC, Baltimore, pp. 85–121.

Johnson, K.S., Gordon, R.M., Coale, K.H., 1997. What controls dissolved iron concentrations in the world ocean? Marine Chemistry 57, 137–161.

Jones, G.J., Palenik, B.P., Morel, F.M.M., 1987. Trace metal reduction by phytoplankton: the role of plasmalemma redox enzymes. Journal of Phycology 23, 237–244.

King, D.W., Aldrich, R.A., Charnecki, S.E., 1993. Photochemical redox cycling of iron in NaCl solutions. Marine Chemistry 44, 105–120.

Kirchman, D.L., Rich, J.H., Barber, R.T., 1995. Biomass and biomass production of heterotrophic bacteria along 140°W in the equatorial pacific—effect of temperature on the microbial loop. Deep-Sea Research II 42 (2–3), 603–619.

Kremling, K., Streu, P., 1993. Saharan dust influenced trace element fluxes in deep North Atlantic subtropical waters. Deep-Sea Research I 40 (6), 1155–1168.

Kuma, K., Nakabayashi, S., Suzuki, Y., Kudo, I., Matsunaga, K., 1992. Photoreduction of Fe(III) by dissolved organic substances and existence of Fe(II) in seawater during spring blooms. Marine Chemistry 37, 15–27.

Kuma, K., Nishioka, J., Matsunaga, K., 1996. Controls on Fe(III) hydroxide solubility in seawater: the influence of pH and natural organic chelators. Limnology and Oceanography 41, 396–407.

Kuma, K., Tanaka, J., Matsunaga, K., 2000. Effect of hydroxamate ferrisiderophore complex (ferrichrome) on iron uptake and growth of a coastal marine diatom, *Chaetoceros sociale*. Limnology and Oceanography 45 (6), 1235–1244.

Laës, A., Blain, S., Laan, P., Achterberg, E.P., Sarthou, G., de Baar, H.J.W., 2003. Deep dissolved iron profiles in the eastern North Atlantic in relation to water masses. Geophysical Research Letters 30 (17).

Landing, W.M., Cutter, G.A., Dalziel, J.A., Flegal, A.R., Powell, R.T., Schmidt, D., Shiller, A., Statham, P., Westerlund, S., Resing, J., 1995. Analytical intercomparison results from the 1990 Intergovernmental Oceanographic Commission open-ocean baseline survey for trace metals: Atlantic Ocean. Marine Chemistry 49, 253–265.

Lenes, J.M., Darrow, B.P., Cattrall, C., Heil, C.A., Callahan, M., Vargo, A.G., Byrne, R.H., Prospero, J.M., Bates, D.E., Fanning, K.A., Walsh, J.J., 2001. Iron fertilization and Trichodesmium response on the West Florida shelf. Limnology and Oceanography 46, 1261–1277.

Maldonado, M.T., Price, N.M., 2000. Nitrate regulation of Fe reduction and transport by Fe-limited *Thalassiosira oceanica*. Limnology and Oceanography 45 (4), 814–826.

Martin, J.H., Fitzwater, S.E., Gordon, R.M., Hunter, C.N., Tanner, S.J., 1993. Iron, primary production and carbon–nitrogen flux studies during the JGOFS North Atlantic Bloom Experiment. Deep-Sea Research II 40, 115–134.

Measures, C.I., Edmond, J.M., 1988. Aluminium as a tracer of the deep outflow from the Mediterranean. Journal of Geophysical Research 93 (C1), 591–595.

Measures, C.I., Yuan, J., Resing, J.A., 1995. Determination of iron in seawater by flow injection-analysis using in-line preconcentration and spectrophotometric detection. Marine Chemistry 50 (1–4), 3–12.

Millero, F.J., 1998. Solubility of Fe(III) in seawater. Earth and Planetary Science Letters 154 (1–4), 323–329.

Millero, F.J., Sotolongo, S., 1989. The oxidation of Fe(II) with H_2O_2 in seawater. Geochimica et Cosmochimica Acta 53, 1867–1873.

Millero, F.J., Sotolongo, S., Izaguire, M., 1987. The oxidation kinetics of Fe(II) in seawater. Geochimica et Cosmochimica Acta 51, 793–802.

Moffett, J.W., Zika, R.G., Brand, L.E., 1990. Distribution and potential sources and sinks of copper chelators in the Sargasso Sea. Deep-Sea Research A 37, 27–36.

Nolting, R.F., Gerringa, L.J.A., Swagerman, M.J.W., Timmermans, K.R., de Baar, H.J.W., 1998. Fe(III) speciation in the high nutrient, low chlorophyll Pacific region of the Southern Ocean. Marine Chemistry 62, 335–352.

Nolting, R.F., Heijne, M., de Jong, J.T.M., Timmermans, K.R., de Baar, H.J.W., 2000. The determination and distribution of Zn in surface water samples collected in the northeast Atlantic Ocean. Journal of Environmental Monitoring 2, 534–538.

O'Sullivan, D.W., Hanson, A.K., Miller, W.L., Kester, D.R., 1991. Measurements of Fe(II) in surface waters of the equatorial Pacific. Limnology Oceanography 36, 1727–1741.

Pérez-Marrero, J., Llinás, O., Maroto, L., Rueda, M.J., Cianca, A., 2002. Saharan dust storms over the Canary Islands during winter 1998 as depicted from the advanced very high-resolution radiometer. Deep-Sea Research II 49, 3465–3479.

Powell, R.T., Donat, J.R., 2001. Distributions of organic Fe complexing ligands in the South and Equatorial Atlantic. Deep-Sea Research II 48 (13), 2877–2893.

Reid, R.T., Live, D.G., Faulkner, D.J., Butler, A., 1993. A siderophore from a marine bacterium with an exceptional ferric ion affinity constant. Nature 366, 455–458.

Rich, H.W., Morel, F.M.M., 1990. Availability of well-defined iron colloids to marine diatom *Thalassiosira weissflogii*. Limnology and Oceanography 35, 652–662.

Rue, E.L., Bruland, K.W., 1995. Complexation of FeIII by natural organic ligands in the Central North Pacific as determined by a new competitive ligand equilibration/adsorptive cathodic stripping voltammetric method. Marine Chemistry 50, 117–138.

Rue, E.L., Bruland, K.W., 1997. The role of organic complexation on ambient iron chemistry in the equatorial Pacific Ocean and the response of a mesoscale iron addition experiment. Limnology and Oceanography 42 (5), 901–910.

Ruzic, I., 1982. Theoretical aspects of the direct titration of natural waters and its information yield for trace metal speciation. Analytica Chimica Acta 140, 99–113.

Santana-Castiano, J.M., Davila, M.G., Rodriguez, M.J., Millero, F.J., 2000. The effect of organic compounds in the oxidation kinetics of FeII. Marine Chemistry 70, 211–222.

Sarthou, G., Baker, A., Blain, S., Achterberg, E.P., Boye, M., Bowie, A.R., Croot, P.L., Laan, P., de Baar, H.J.W., Jickells, T.D., Worsfold, P.J., 2003. Atmospheric iron deposition and sea-surface dissolved iron concentrations in the eastern Atlantic Ocean. Deep-Sea Research 1, 50 (10–11), 1339–1352.

Sulzberger, B., Suter, D., Siffert, C., Banwart, S., Stumm, W., 1989. Dissolution of Fe(III)(hydr)oxides in natural-waters—laboratory assessment on the kinetics controlled by surface coordination. Marine Chemistry 28 (1–3), 127–144.

Sunda, W.G., Huntsman, S.A., 1995. Iron uptake and growth limitation in oceanic and coastal phytoplankton. Marine Chemistry 50, 189–206.

Timmermans, K.R., Gerringa, L.J.A., de Baar, H.J.W., van der Wagt, B., Veldhuis, M.J.W., de Jong, J.T.M., Croot, P.L., Boye, M., 2001. Growth rates of large and small Southern Ocean diatoms in relation to availability of iron in natural seawater. Limnology and Oceanography 46 (2), 260–266.

Timmermans, K.R., van der Wagt, B., Veldhuis, M.J.W., Maatman, A., de Baar, H.J.W., 2005. Physiological responses of three species of marine pico-phytoplankton to ammonium, phosphate, iron and light limitation. Journal of Sea Research 53 (1–2), 109–120.

Torres-Padrón, M.E., Gelado-Caballero, M.D., Collado-Sanchéz, C., Siruela-Matos, V.F., Cardona-Castellano, P.J., Hernández-Brito, J.J., 2002. Variability of dust inputs to the CANIGO zone. Deep-Sea Research II 49, 3455–3464.

Trick, C.G., Wilhelm, S.W., 1995. Physiological changes in the coastal marine cynobacterium *Synechococcus* sp., PCC-7002 exposed to low ferric ion levels. Marine Chemistry 50, 207–217.

Van den Berg, C.M.G., 1982. Determination of copper complexation with natural organic ligands in seawater by equilibration with MnO_2. Marine Chemistry 11, 307–322.

Van den Berg, C.M.G., 1995. Evidence for organic complexation of iron in seawater. Marine Chemistry 50, 139–157.

Van den Berg, C.M.G., Kramer, J.R., 1979. Determination of complexing capacities and conditional stability constants for copper in natural waters using MnO_2. Analytica Chimica Acta 106, 113–120.

Veldhuis, M.J.W., Kraay, G.W., 2004. Phytoplankton in the subtropical Atlantic Ocean: towards a better assessment of biomass and composition. Deep-Sea Research I 51 (4), 507–530.

Visser, F., Gerringa, L.J.A., Van der Gaast, S.J., de Baar, H.J.W., Timmermans, K.R., 2003. The role of the reactivity and content of iron of aerosol dust on growth rates of two Antarctic diatom species. Journal of Phycology 39 (6), 1085–1094.

Voelker, B.M., Sedlak, D.L., 1995. Iron reduction by photoproduced superoxide in seawater. Marine Chemistry 50 (1–4), 93–102.

Waite, T.D., Szymczak, R., Esprey, Q.I., Furnas, J.M., 1995. Daily variations in iron speciation in northern Australian shelf waters. Marine Chemistry 50, 79–92.

Wilhelm, S.W., Trick, C.G., 1994. Iron-limited growth in cyanobacteria: siderophore production is a common response. Limnology and Oceanography 39, 1979–1984.

Wilhelm, S.W., Trick, C.G., 1995. Physiological profiles of *Synechococcus* (Cyanophyceae) grown in iron-limited continuous culture. Journal of Phycology 31, 79–85.

Witter, A.E., Luther, G.W., 1998. Variation in Fe-organic complexation with depth in the Northwestern Atlantic Ocean as determined using a kinetic approach. Marine Chemistry 62, 241–258.

Wu, J., Luther III, G.W., 1995. Complexation of Fe(III) by natural organic ligands in the Northwest Atlantic Ocean by competitive ligand equilibration method and a kinetic approach. Marine Chemistry 50, 159–178.

Wu, J.F., Boyle, E., Sunda, W., Wen, L.S., 2001. Soluble and colloidal iron in the olgotrophic North Atlantic and North Pacific. Science 293 (5531), 847–849.

Young, R.W., Crader, K.L., Betzer, P.R., Costello, D.K., Duce, R.A., DiTullio, G.R., Tindale, N.W., Laws, E.A., Uematsu, M., Merrill, J.T., Feeley, R.A., 1991. Atmospheric iron inputs and primary productivity: phytoplankton responses in the North Pacific. Global Biogeochemical Cycles 5, 119–134.

Zhuang, G.S., Yi, Z., Wallace, G.T., 1995. Fe(II) in rainwater, snow, and surface seawater from a coastal environment. Marine Chemistry 50 (1–4), 41–50.